doi.org/10.1002/batt.202100208

The Origin of Gaseous Decomposition Products Formed During SEI Formation Analyzed by Isotope Labeling in Lithium-Ion Battery Electrolytes

Marco Leißing,[a] Christoph Peschel,[a] Fabian Horsthemke,[a] Simon Wiemers-Meyer,[a] Martin Winter,[a, b] and Sascha Nowak*[a]

Interphase formation during the first charge and discharge cycle(s) of a battery cell is among the least understood processes in lithium-ion batteries (LIBs). The formation of interphases is a result of electrolyte decomposition and accompanied by gassing. The direct analysis of these interphases is challenging and indirect methods are required to obtain information about this process. For example, indirect, *ex situ* analyses of gaseous decomposition products can help to draw conclusions about occurring reactions in the cell. In this work, the origin of several permanent gases and hydrocarbons (CO, CH_4, C_2H_4 and C_2H_6) emerging during the formation of $LiNi_{0.6}Mn_{0.2}Co_{0.2}O_2$ (NMC622)||graphite pouch type LIBs equipped with a gas sampling port was investigated. Isotope labeled electrolytes ($^{13}C_3$-EC, D_4-EC) were used to assign formation gas products to the individual constituents of the electrolyte mixture. The effect of common linear carbonates in combination with ethylene carbonate (EC) as well as the effect of vinylene carbonate (VC) as film forming additive was investigated. The obtained mass spectra from gas chromatography mass spectrometry (GC-MS) and the mass shift caused by the labeled electrolyte components, enabled an assignment of individual electrolyte components to the resulting gas products. The aim of this work is to gain more information about interphase reactions and thus to improve understanding of the mechanisms behind formation.

1. Introduction

Lithium-ion batteries (LIBs) are the first choice for mobile electronic devices and an important technology for todays and future mobility.[1,2] Still, many processes in LIBs are scientifically not fully understood. Especially, the investigation of the formation of protective layers (=interphases) between the electrodes and the electrolyte during the first charge and discharge cycle(s) of a battery cell is of enormous interest in research.Appropriate formation of these interphases, *i.e.* of the so called solid-electrolyte interphase (SEI) on the negative electrode side and the cathode electrolyte interphase (CEI) on the positive electrode side, is mandatory for long-term performance and safety of the battery cell.[3–7]

A state-of-the-art LIB consists of a negative electrode, commonly graphite-based and a positive electrode, typically a lithium transition metal oxide.[8] In between, a separator provides electronic insulation, which is wetted with liquid organic electrolyte.[9] The electrolyte consists of a conducting salt, most common lithium hexafluorophosphate ($LiPF_6$) which is dissolved in a mixture of linear (*e.g.* dimethyl carbonate (DMC), ethyl methyl carbonate (EMC) and diethyl carbonate (DEC)) with cyclic organic carbonates (*e.g.* ethylene carbonate (EC)).[10,11] Film forming additives such as vinylene carbonate (VC) are commonly added to the electrolyte to increase the overall performance of LIBs due to an advantageous effect on the SEI and/or CEI formation.[12–15] The conception of the SEI, which is built up in a kind of mosaic structure, is widely accepted. Close to the negative electrode surface, species like Li_2O, Li_2CO_3, and LiF are present in compact layers. In the direction of the electrolyte, organic electrolyte decomposition products such as oligomer species and semicarbonates are more abundant.[16–19] However, the reductive atmosphere at the anode forms not only organic and inorganic products that result in the SEI, but also gaseous decomposition products that result from the electrolyte.[3–5,20] However, the low thickness as well as the low stability of the SEI towards current sampling and surface analysis techniques makes a direct, *in situ* or *operando* analysis challenging.[19,21] A detour *via post mortem* extraction and investigation of the decomposition products can enable deeper insights in the process of electrolyte decomposition.[22,23] Chromatographic methods *e.g.* gas chromatography (GC) were widely utilized for the analysis of the liquid and gaseous analytes.[24] Gases *e.g.* H_2, CO, CO_2, CH_4, C_2H_4 and C_2H_6 were identified and quantified in the formation gas.[25–38] Moreover, application of isotope labeled electrolytes offers the possibility to clarify decomposition pathways and

[a] M. Leißing, C. Peschel, F. Horsthemke, S. Wiemers-Meyer, M. Winter, Dr. S. Nowak
University of Münster, MEET Battery Research Center, Corrensstraße 46, 48149 Münster, Germany
E-mail: sascha.nowak@uni-muenster.de
[b] M. Winter
Helmholtz-Institute Münster, IEK-12, Forschungszentrum Jülich, Corrensstraße 46, 48149 Münster, Germany

Supporting information for this article is available on the WWW under https://doi.org/10.1002/batt.202100208

assign reaction products to certain electrolyte components.[26,28,39–41] Onuki *et al.* used $^{13}C_3$-EC and $^{13}C_5$-DEC as part of the electrolyte to confirm *inter alia* the reaction of EC forming C_2H_4 in LIBs.[28]

This publication is part of a series of studies on isotopically labeled electrolytes, which in this case focuses not on the liquid, but particularly on the gaseous products formed during formation.[40,41] Except for a few gaseous products like C_2H_4, where some studies indicate their origin, the data situation for several other gaseous decomposition products are insufficient and many proposed decomposition pathways in LIB are based on mechanistic conclusions rather than true analytical evidence.[4,42] This study aims to contribute more experimental data to the discussion. Therefore, the reactions of EC-based electrolytes with three common linear carbonates (DMC, EMC and DEC) as well as the influence of VC are thoroughly investigated and summarized. $^{13}C_3$-EC and D_4-EC were used to confirm the origin of C-atoms and H-atoms in the respective gas components after formation cycles.

Experimental Section

Chemicals

The organic carbonates DMC (99.0%), EMC (99.99%) and DEC (99.98%) as well as the conducting salt $LiPF_6$ (99.8%) were obtained from BASF (Germany). $^{13}C_3$-EC (99% ^{13}C, 97%) and D_4-EC (98% D_4, 99%) purchased from Sigma Aldrich (Germany) and EC (99.99%) was purchased from Targray (Canada). The electrolytes were automatically mixed using a high throughput screening (HTS) robot. Labeled EC was added manually.

Electrolyte formulation, cell assembly and electrochemical cell formation

Commercially available, electrolyte free NMC622||graphite two electrode[43] LIB pouch cells (Li-Fun Technology, China) were cut open and dried in a vacuum oven for 24 h at 60 °C. Following a gas sampling port (GSP) was placed between the pouch foil and fixed by heat-sealing (195 C, 20 s). The cells were filled with 700 µL of the respective electrolyte formulation (Table 1) *via* GSP. Following the cell was cut open to enable vacuum-sealing at 165 °C and a relative pressure of −90 kPa for 5 s. For detailed description of the cell preparation and the GSP the reader is kindly referred to Schmiegel *et al.*[29]

After wetting for 20 h, two constant current/constant voltage (CC/CV) charge (0.2 C; < 0.05 C) and CC discharge (0.2 C) cycles were performed in a voltage window between 3.0 and 4.2 V.[41] After formation, the emerged gas was directly extracted from the cell *via* GSP and injected to the GC system. The results of the DEC containing electrolyte are discussed in the main part of this paper, mass spectra (MS) of DMC and EMC containing electrolytes can be found in the supporting information.

Table 1. Electrolyte formulations as described were produced by HTS. $^{13}C_3$-EC and D_4-EC were added manually to the premixed electrolyte. All formulations contained 1 molL^{-1} $LiPF_6$ in the respective electrolyte. For the MS of the DMC and EMC containing electrolyte the reader is kindly referred to the supporting information.

Abbreviation	Cyclic carbonate	Linear carbonate	Ratio	Additive
EL_{DEC}	EC	DEC	3/7	–
$EL_{DEC,lab}$	$^{13}C_3$-EC	DEC	3/7	–
$EL_{DEC,lab\ D4}$	D_4-EC	DEC	3/7	–
$EL_{DEC+VC,lab}$	$^{13}C_3$-EC	DEC	3/7	2 w% VC
EL_{DMC}	EC	DMC	3/7	–
$EL_{DMC,lab}$	$^{13}C_3$-EC	DMC	3/7	–
EL_{EMC}	EC	EMC	3/7	–
$EL_{EMC,lab}$	$^{13}C_3$-EC	EMC	3/7	–
$EL_{DMC+VC,lab}$	$^{13}C_3$-EC	DMC	3/7	2 w% VC
$EL_{EMC+VC,lab}$	$^{13}C_3$-EC	EMC	3/7	2 w% VC

Gas chromatography

All gas GC-MS measurements were performed using a GCMS-QP2010 Ultra system (Shimadzu, Germany). A PLOT gas separation column RT®-Msieve 5 A (30 m × 0.32 mm × 30 µm; Restek, Germany) was used for the separation of permanent gases and hydrocarbons. GC and mass spectrometer settings were applied according to literature.[30] The fitting of fragment intensities observed from GC-MS results is described in the supporting information.

The liquid measurements were executed on the same GC device with assembled AOC-5000 Plus autosampler (Shimadzu, Germany) and a nonpolar Supelco SLB®-5 ms (30 m × 0.25 mm × 0.25 µm, Sigma Aldrich) column. Further parameters and sample preparation conditions were applied according to Horsthemke et al.[44,45]

2. Results and Discussion

$^{13}C_3$-EC and D_4-EC were used as part of the electrolyte to assign the individual gaseous products to the respective carbonate solvent by GC-MS. The $^{13}C_3$-labeling provides information about the origin of C-atoms and the D_4-labeling about the origin of the H-atoms in the respective decomposition species. In the main part, the focus was set to an electrolyte system which consists of EC, DEC and the conducting salt $LiPF_6$.

For an unambiguous assignment of the gaseous decomposition products to their molecular origin it is crucial to exclude the reaction of labeled EC and unlabeled DEC solvent reagents resulting in mixed labeled intermediates during the formation process in the liquid electrolyte. Figure S1 depicts the GC-MS fragment patterns of unlabeled EC, D_4-EC in the fresh electrolyte and D_4-EC after formation as well as the unlabeled pristine and aged DEC. The GC-MS results show that both electrolyte solvents were unaltered after the formation process and no exchange of D-atoms was observed. The same also applies to $^{13}C_3$-EC.[40] Therefore, observable mass shifts of decomposition species caused by labeled atoms can distinctly be referred to an EC origin, whereas unlabeled fragments are DEC-based. Based on this conclusion, the gas phase emerging during the formation process was analyzed by GC-MS to decipher the origin of C- and H-atoms in the respective gaseous decomposition products. In the following, the MS data of the respective component observed from the unlabeled electrolyte (blue) is compared to the component observed from the labeled electrolyte (grey: $^{13}C_3$-EC, orange: D_4-EC). The results for further common electrolytes containing DMC and EMC as linear carbonates are discussed in the chapters and obtained data can be found in the supporting Information. The influence of

VC (green: $^{13}C_3$-EC + VC) as film forming additive in the electrolyte is also discussed in the supporting information.

In the following sections, the gases C_2H_4, CO, CH_4, and C_2H_6 are investigated in detail. It must be noted, that H_2 and CO_2 were identified as decomposition products in several measurements but were not evaluated in this work due to column limitations.

2.1. Ethene

C_2H_4 is a well investigated decomposition product of carbonate-based LIB electrolytes and was assigned to the decomposition of EC on graphite.[28,35,37,46,47] With the obtained mass spectra shown in Figure 1 (top) it was possible to confirm the results from literature for the EL_{DEC} and $EL_{DEC,lab}$ containing cells. The molecular ion $C_2H_4^+$ was shifted from *m/z* 28 (blue) to *m/z* 30 ($^{13}C_2H_4^+$, grey) in the labeled electrolyte, indicating the presence of two ^{13}C-labeled C-atoms in C_2H_4 which originate form EC. The mass shift of +2 Da with comparable intensities was also found for the fragments. The low intensity at *m/z* 29 in the unlabeled electrolyte can be referred to the natural isotope distribution of the C-atom. The natural ratio of $^{13}C/^{12}C$ is approx. 1 %.

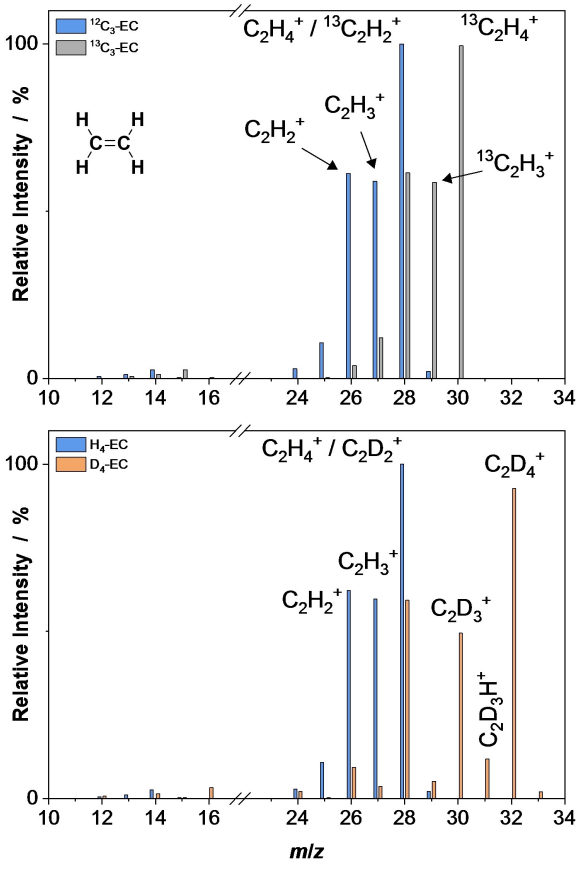

Figure 1. MS of C_2H_4 obtained from cells with EL_{DEC} (blue)/$EL_{DEC,lab}$ (grey, top) and cells with EL_{DEC} (blue)/$EL_{DEC,lab\ D4}$ (orange, bottom) after formation.

C_2H_4 showed the same labeling behavior in the DMC and EMC containing electrolyte. Therefore, the C_2H_4 formation during cell formation is independent on the applied linear carbonate. For the mass spectra of the DMC (EL_{DMC}, $EL_{DMC,lab}$; Figure S4a) and EMC (EL_{EMC}, $EL_{EMC,lab}$; Figure S5a) containing electrolyte the reader is kindly referred to the supporting information.

In Figure 1 (bottom) a notable intensity at *m/z* 32 was observed for the D_4-EC containing electrolyte. The shift of 4 Da starting from the molecular ion at *m/z* 28 ($C_2H_4^+$) indicates a significant presence of the molecular ion $C_2D_4^+$ (*m/z* 32) in the labeled electrolyte system $EL_{DEC,lab\ D4}$ (orange). This shows that the origin of H-atoms in C_2H_4 is just mainly, but not solely EC based, which is in contrast to previous literature, where it is proposed the C_2H_4 is completely stemming from EC. The two main fragments in the reference system $C_2H_3^+$ (*m/z* 27) and $C_2H_2^+$ (*m/z* 26) result from a loss of one or two H-atoms during fragmentation of the molecular ion. Since the D-atoms have the double atomic weight, the loss of one D-atom is indicated by the loss of 2 Da. Therefore, the two main fragments of the D-labeled electrolyte can be found at *m/z* 30 ($C_2D_3^+$) and *m/z* 28 ($C_2D_2^+$), respectively. The ion at *m/z* 31 cannot be a fragment of $C_2D_4^+$ due to the odd *m/z* value. For this reason, a second molecular ion with one H-atom instead of a D-atom ($C_2D_3H^+$) must be present. The relative amount of $C_2D_3H^+$ compared to the main molecular ion $C_2D_4^+$ is small but this indicated the formation of an intermediate, which consists of an additional H-atom originating from DEC. The following reaction [Eq. (1)] depicts the proposed EC decomposition resulting in C_2D_3H. Labeled D-atoms from D_4-EC are marked in red.

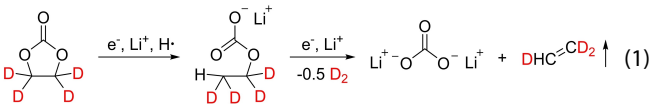

(1)

2.2. Carbon Monoxide

In Figure 2 the MS of CO from both cells EL_{DEC} and $EL_{DEC,lab}$ is depicted. A mass shift of the molecular ion CO^+ from *m/z* 28 to *m/z* 29 in the labeled electrolyte was observed. The high intensity of the labeled $^{13}CO^+$ (*m/z* 29) indicates that most of the C-atoms in CO originated from EC. Nevertheless, also a notable signal with a relative intensity of approx. 20 % was observed at *m/z* 28 from the labeled cells. Since the labeled $^{13}CO^+$ cannot form a fragment at *m/z* 28 the intensity ratio (*m/z* 28/29) directly represents the carbon atom origin resulting from DEC and EC (approx. 20/80). For both carbonate solvents decomposition pathways resulting in CO evolution during formation were proposed in literature.[28,47]

Nevertheless, it was found that the ratio of the solvent decomposition, resulting in CO is dependent on the applied linear carbonate. In the EMC containing electrolyte system (EL_{EMC}, $EL_{EMC,lab}$; Figure S5b) a comparable ratio of CO resulting from EMC and EC was identified. Other than for the ethyl group containing linear carbonate systems, the ratio in the solely

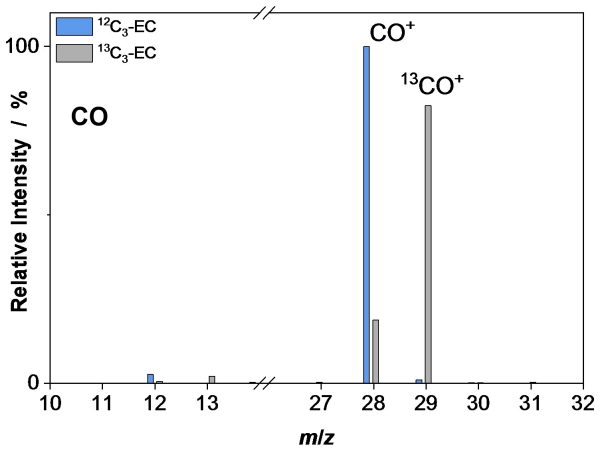

Figure 2. MS of CO obtained from cells with EL_{DEC} (blue) and $EL_{DEC,lab}$ (grey) after formation.

methyl group containing system (EL_{DMC}, $EL_{DMC,lab}$; Figure S4b) was affected. The relative number of C-atoms resulting from linear carbonate was increased and roughly estimated to 35%. Hence, it seems necessary to make a difference for the decomposition reactions resulting in CO if the linear carbonate involve solely methyl or also additionally contains ethyl groups. Overall, the origin of CO was mainly EC-based. In all analysed electrolyte formulations, unlabeled CO (*m/z* 28) was found up to a ratio of 1/3 in the total CO intensity and therefore assigned to linear carbonate decomposition.

According to literature, CO forming reactions of the linear [Eq. (2)][28] and cyclic [Eq. (3)][47] carbonates were considered in the following reactions ($R_{1,2}$=CH_3 and/or C_2H_5):

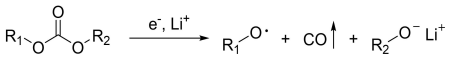

(2)

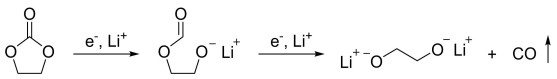

(3)

With the results in this study, we confirm that both carbonates form CO during decomposition. Nevertheless, the decomposition of EC to CO was found to be preferred compared to the linear carbonates.

2.3. Methane

The MS of CH_4 obtained from cells with EL_{DEC} and $EL_{DEC,lab}$ after formation is shown in Figure 3 (top). The molecular ion peak for the unlabeled component (EL_{DEC}) with highest intensity can be found at a *m/z* 16 (CH_4^+). In the labeled electrolyte ($EL_{DEC,lab}$) a shift of 1 Da to *m/z* 17 ($^{13}CH_4^+$) was observed with a relative intensity of approx. 60% after correction. This indicates a second, unlabeled molecular ion overlaying with the labeled fragment after loss of a hydrogen atom at *m/z* 16 ($^{13}CH_3^+$). The unlabeled component with DEC origin increases the signal at

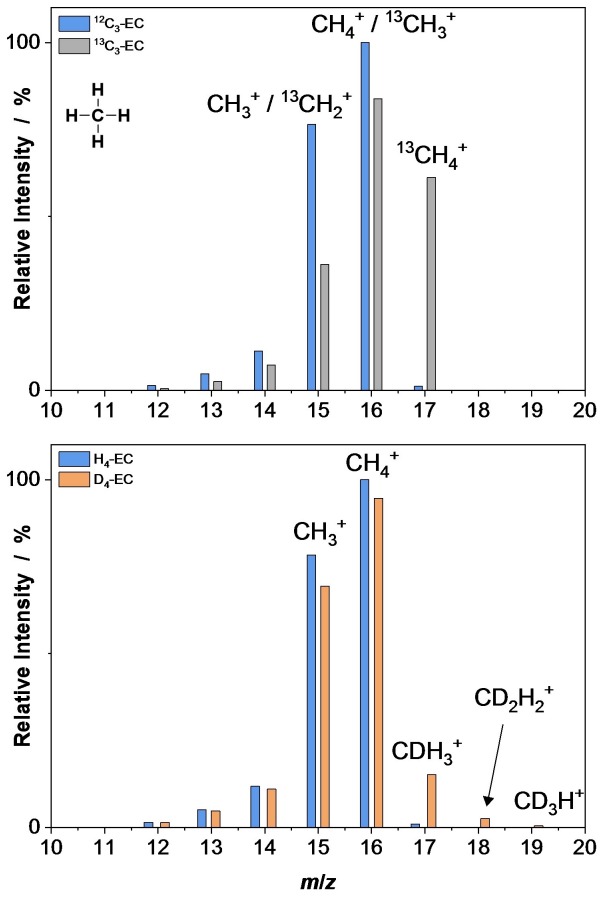

Figure 3. MS of CH_4 obtained from cells with EL_{DEC} (blue)/$EL_{DEC,lab}$ (grey, top) and with EL_{DEC} (blue)/$EL_{DEC,lab\ D4}$ (orange, bottom) after formation.

m/z 16. The presence of unlabeled CH_4 was also indicated by a relatively high intensity at *m/z* 15 (CH_3^+). Furthermore, the undisturbed signal with a relative intensity more than 60% at *m/z* 17, represents the molecular ion $^{13}CH_4^+$ resulting from EC. Hence, the origin of the C-atom in CH_4 was EC- and DEC-based, whereby EC was slightly preferred.

Nevertheless, C-atom origin in CH_4 depends on the applied linear carbonate in the electrolyte. The more methyl groups in the linear carbonate (DMC > EMC > DEC), the higher the share of unlabeled, linear carbonate-based C-atoms in CH_4. The presence of methyl groups in the linear carbonate could decrease the relative intensity of the $^{13}CH_4^+$-ion to 25% with EMC (EL_{EMC}, $EL_{EMC,lab}$; Figure S5c) and to 5% relative intensity with DMC (EL_{DMC}, $EL_{DMC,lab}$; Figure S4c).

In contrast to the C-atom in CH_4, the origin of the H-atoms can be mainly assigned to the linear carbonate DEC. The highest intensity in the unlabeled (EL_{DEC}) and labeled ($EL_{DEC,\ lab\ D4}$) electrolyte was observed for *m/z* 16 (CH_4^+; Figure 3 bottom). Only low intensities were found for higher *m*/z-values. Nevertheless, *m/z* 19 provided the presence of the molecular ion CD_3H^+ which was predominantly expected with respect to the C-atom origin in CH_4. The molecular ion at *m/z* 19 (CD_3H^+) with 3 D-atoms indicates the uptake of one H-atom from the linear carbonate. Higher relative intensities were observed for *m/z* 18 ($CD_2H_2^+$) and *m/z* 17 (CDH_3^+) which mainly result from the

molecular ions but also from fragments. The pronounced intensity at *m/z* 16 (approx. 95%) is mainly caused by CH_4^+ molecular ions but the fragments CDH_2^+ and CD_2^+ can also contribute to the measured intensity. However, considering the fragmentation pattern of the unlabeled component, this part can be as high as 15%.

In literature, several reactions of the linear [Eq. (4)][47,48] and the cyclic [Eqs. (5, 6)][25,49] carbonate were described resulting in CH_4 as decomposition product ($R_{1,2}$ = –CH_3):

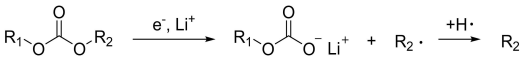

(4)

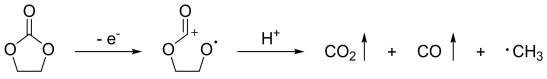

(5)

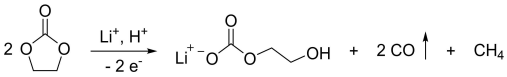

(6)

Ota et al. investigated an EC/DMC based electrolyte and identified the linear carbonate as the source of CH_4. This was proposed based on the absence of CH_4 in the solely EC-based electrolyte. The linear carbonate can form a methyl radical, which following reacts with a hydrogen atom to form CH_4.[47] Metzger et al. proposed a mechanism for the EC decomposition, were methyl radicals can occur.[25] After abstraction of a hydrogen atom this would also result in CH_4 evolution. Hobold et al. recently proposed the reaction of two EC molecules forming lithium ethylene monocarbonate (LEMC), CO and CH_4.[49]

Based on the obtained mass spectra results for the origin of C- and H-atoms in CH_4, a more complex reactivity forming CH_4 in EL_{DEC} has to be considered. The C-atom origin of CH_4 was mainly found to be EC-based whereas the H-atoms were concluded as DEC-based. Since the origin of H-atoms was not focused in the literature so far, it was widely accepted that the hydrogen atoms retain their bond to the respective C-atom during decomposition. The present results indicate that the electrolyte decomposition and mechanism of gassing during SEI formation is subject to a series of reactions forming CH_4. In the experiment, the existing bonds between D-atoms and C-atoms were cleaved and new bonds to H-atoms originating from the DEC were formed. This process seems to be favored compared to the straight reaction without the exchange of H-atoms, which, was intuitively suspected. Hence, the processes are not trivial and require further investigation. The elucidation of these processes is essential for a basic understanding of SEI and its formation.

2.4. Ethane

In Figure 4 (top) the MS of ethane (C_2H_6) from EL_{DEC} and $EL_{DEC,lab}$ is depicted. C_2H_6 consists of two C-atoms which enables a maximum mass shift of +2 Da for the ^{13}C-labeled component.

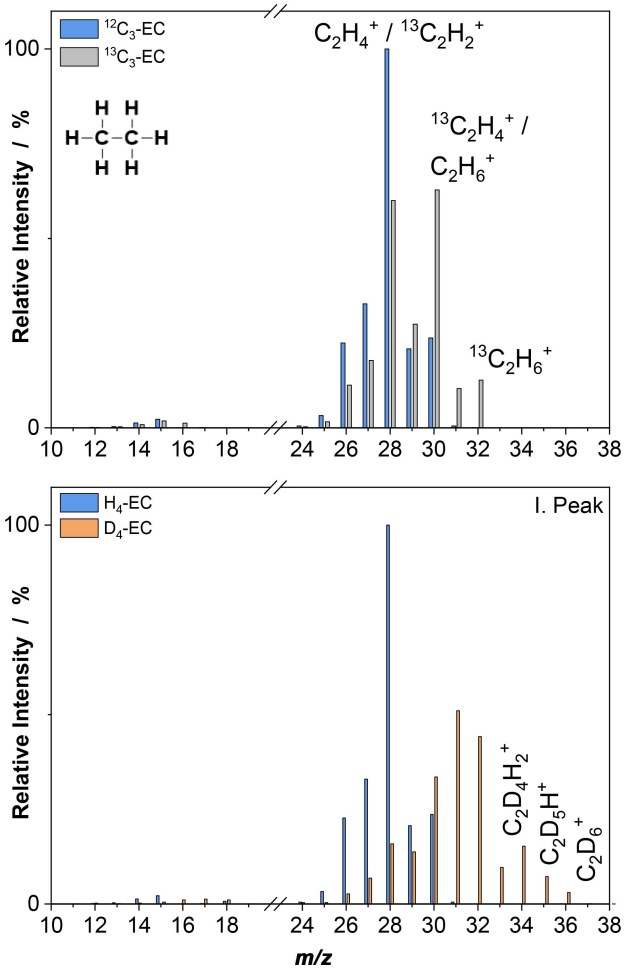

Figure 4. MS of C_2H_6 observed from cells with EL_{DEC} (blue)/$EL_{DEC,lab}$ (grey, top) and the first peak of EL_{DEC} (blue)/$EL_{DEC,lab\ D4}$ (orange, bottom) after formation.

This shift of +2 Da for the molecular ion ($C_2H_6^+$) from *m/z* 30 for the unlabeled component to *m/z* 32 ($^{13}C_2H_6^+$) for the labeled component was observed. This indicates that C_2H_6 is partially EC-based. The loss of two H-atoms during fragmentation, starting from the labeled component, results in a fragment with the highest intensity at *m/z* 30 ($^{13}C_2H_4^+$) in the MS.

Nevertheless, a relative high intensity for *m/z* 28 in the labeled electrolyte indicates the presence of unlabeled C_2H_6 in the gas phase. Due to the overlay of fragments and molecular ions at *m/z* 28 ($^{13}C_2H_2^+$, $C_2H_4^+$) and *m/z* 30 ($^{13}C_2H_4^+$, $C_2H_6^+$) the intensities cannot be entirely traced back to the exact contribution of the solvent molecules. However, a contribution of EC-based decomposition resulting in C_2H_6 was proven.

For the DMC-based electrolyte an increased EC decomposition compared to the DEC-based electrolyte was observed (EL_{DMC}, $EL_{DMC,lab}$; Figure S4d). The origin of C-atoms in C_2H_6 resulting from the linear carbonate was increased if EMC (EL_{EMC}, $EL_{EMC,lab}$; Figure S5d) was used instead of DMC or DEC. The asymmetric structure of EMC with ethyl and methyl group seems to have an influence on the reaction and the formation of C_2H_6.

The total ion chromatogram (TIC) observed from the cells filled with $EL_{DEC,lab\ D4}$ showed two peaks in the retention time window of C_2H_6 (Figure S2). Both peaks represent the analyte C_2H_6 but, in this case, the labeled and unlabeled molecules appear chromatographically separated. The first peak contained more labeled components (Figure 4 bottom) and the second mainly unlabeled components (Figure S3). The molecules in the first peak showed less interaction with the column, which in the following resulted in a slightly shorter retention time for the labeled components.

Since the origin of the D-atoms can be assigned to the labeled D_4-EC, it is reasonable to assume that the origin of the C-atoms in the first peak is also EC based. The C-atoms in the second peak, which is mostly unlabeled, originate from DEC. This assumes that the exchange of all D-atoms from the labeled EC is unlikely. With these assumptions and the areas from the TIC chromatogram, the ratio of C_2H_4 resulting from EC was estimated to be 1/3 and from DEC to be 2/3.

The lowered normalized intensities and the broader *m/z* distribution observed from C_2H_6 and the first peak (RT = 13.74 min) indicate that several molecular ions must be present (Figure 4 bottom). From the signals at *m/z* 36 and *m/z* 35 the molecular ions $C_2D_6^+$ and $C_2D_5H^+$ were identified. These signals are undisturbed by other fragment ions. Therefore, a higher content of C_2D_5H molecules compared to C_2D_6 was concluded. The possible molecular ion $C_2D_4H_2^+$ was identified at *m/z* 34 which overlaid by the fragment $C_2D_5^+$ from the molecular ions $C_2D_6^+$ (loss of D, −2 Da) and $C_2D_5H^+$ (loss of H, −1 Da). Further molecular ions are possible, but were not found in a noteworthy amount.

In summary, the molecular ions $C_2D_6^+$, $C_2D_5H^+$ and $C_2D_4H_2^+$ are the main molecular ions to consider. In the mass spectra of the reference electrolyte the fragment with the loss of −2 H-atoms shows the highest intensity. With this in mind the probability for ions at *m/z* 32 in the $EL_{DEC,lab\ D4}$ system is high, because the loss of two D-atoms and/or H-atoms starting from the molecular ions would result in *m/z* 32 for each molecular ion. However, the intensity for *m/z* 31 is highest which proves that the formation of $C_2D_5H^+$ is preferred compared to $C_2D_4H_2^+$ and $C_2D_6^+$.

Altogether, the first fraction composes mainly of three different molecules (C_2D_6, C_2D_5H, $C_2D_4H_2$). Hence, during the decomposition of EC reactions with H-atoms from EC or DEC have to be considered for C_2H_6 formation. Nevertheless, the amount of C_2H_6 molecules originate from DEC is higher than from EC. DEC-based molecules solely react with H-atoms from DEC with negligible exception.

A commonly described mechanism of the linear carbonate [Eq. (7)][27,50–52] decomposition resulting in C_2H_6 is redrawn in the following reaction scheme ($R_{1,2}$ = –CH_3):

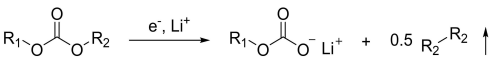

(7)

Reaction scheme (4) also depicts the decomposition reaction, which results in C_2H_6. Instead of CH_3-radicals forming CH_4, C_2H_5-radical abstract a H-radical and form C_2H_6. Furthermore, the analogous decomposition reaction of EC mentioned in reaction scheme (5) would also result in the formation of C_2H_6 after recombination of two CH_3-radicals.

The performed experiments can confirm the described decomposition reactions of the linear carbonate forming C_2H_6. However, the recombination of two CH_3-radicals resulting from the linear carbonate seems to be the most probable one. Secondly, the recombination of a C_2H_5-radical with a hydrogen radical. The lower probability is supported by the fact that the formation of C_2H_5-radicals is lower than that of CH_3-radicals since the decomposition of EMC was found to be preferred to DMC. Therefore, the CH_3-radical seems to be the leaving group and the molecule is stabilized by the larger C_2H_5-group. Furthermore, the fact that selective H-radicals from the linear carbonate were found to form C_2H_6 excludes C_2H_5- as a leaving group.

Nevertheless, also the decomposition of EC resulted in C_2H_6 and the gas evolution reactions seems to be more complex than described in literature. The hydrogen exchange reactions reported in this study can result from the following proposed reaction [Eq. (8)]. Labeled deuterium atoms from D_4-EC are marked in red:

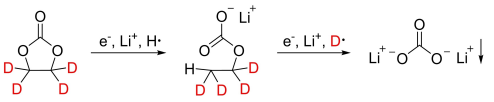

(8)

In Table 2 and Table 3, the origin of the C-atoms and H-atoms in the gaseous analyte resulting from the respective electrolyte mixture after formation is concluded. The x marks the carbonate which is solely the origin of the respective analyte. Arrows indicate a higher decomposition of the respective carbonate if one is preferred.

Figure 5 summarizes the results observed from experiments using isotope labeled $^{13}C_3$-EC and the effect of VC as film forming additive on the origin of gaseous decomposition products. A detailed consideration of the results obtained for the different electrolyte systems with the addition of VC can be found in the supporting information. The graph shows by

Table 2. Origins of C-atoms in electrolyte formulations with DMC, EMC or DEC as linear carbonate and EC as cyclic carbonate. The x marks the origin of the respective analyte. The arrows indicate from which carbonate the gas originated to a larger extent if it results from both carbonates.

Linear carbonate		EL_{DMC}			EL_{EMC}			EL_{DEC}	
Analyte	EC	Both	DMC	EC	Both	EMC	EC	Both	DEC
Ethene	x			x			x		
Carbon monoxide		←			←			←	
Methane			x		→			←	
Ethane		←			→			x	

Table 3. Origins of H-atoms in electrolyte formulations with DEC as linear carbonate and EC as cyclic carbonate. The x marks the origin of the respective analyte. The arrows indicate from which carbonate the gas originated to a larger extent if it results from both carbonates.

Linear carbonate		EL_{DEC}	
Analyte	EC	Both	DEC
Ethene	x		
Methane			x
Ethane		→	

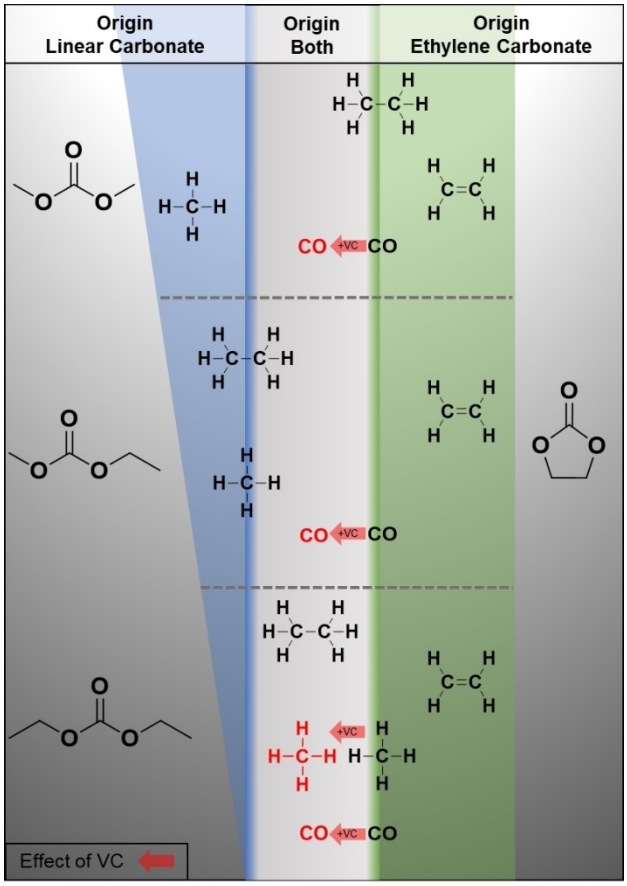

Figure 5. The figure shows the solvent origins of C-atoms in gaseous decomposition products observed from electrolyte formulations with DMC, EMC or DEC (left side) as linear carbonate and EC (right side) as cyclic carbonate after formation. The position of the gaseous decomposition product in *x*-dimension indicate the linear or cyclic carbonate origin of the respective analyte. A distinction is made between exclusively resulting from the linear carbonate (blue area), from both carbonates (middle, grey area), from both carbonates with the respective preferred carbonate (border between the blue I grey or grey I green area) and exclusively from EC (green area). The red arrows indicate the effect of VC as film forming additive on the respective decomposition product origin compared to the VC free electrolyte.

position of the decomposition product whether it is exclusively resulting from the linear carbonate (blue area), from ethylene carbonate (green area) or from both carbonates to equal parts (middle, grey area). The decomposition product can also be placed on the border between the blue/grey or grey/green area when the decomposition product is in general resulting from both carbonates but preferably resulting from a certain carbonate. In addition to the comprehensively studied decomposition product C_2H_4, which is formed mainly from EC, the origin of CH_4 and C_2H_6 can vary with the linear carbonate used in the electrolyte. The origin of CO is mostly EC based, whereas the use of the additive VC in the electrolyte increases the proportion of linear carbonate or respectively decreases the proportion of EC. Thus, CO is formed in equal parts from linear carbonate and EC, as shown by the red arrow. Furthermore, the use of VC affects CH_4 formation from the DEC based electrolyte in the same way (red arrow). The decomposition of other components is not notably affected by VC.

3. Conclusions

In this study, gaseous decomposition products evolving during the LIB cell formation process were investigated and assigned to their electrolytic origin. Several state-of-the-art electrolytes containing either DEC, DMC or EMC in combination with EC were examined. For convenient gas extraction, commercially available pouch type NMC622||graphite LIB cells were equipped with a gas sampling port (GSP). To follow the decomposition reaction during formation, EC was stepwise replaced by labeled ^{13}C-EC and D_4-EC. The resulting formation gas was extracted *via* the GSP and validated by GC-MS. Shifts in the observed mass spectra showed the presence of the respective labeled formation gas component originating from the labeled EC. The extracted gas phase consisted of H_2, C_2H_4, CO, CH_4, C_2H_6 and CO_2 after formation.

It was proven, that the origin of the C-atoms of C_2H_4 formed in the DEC/EC electrolyte could be solely assigned to EC, which is literature known. Nevertheless, it was assumed in previous literature that also the H-atoms in C_2H_4 solely originate from the EC. However, with labeled D_4-EC it was possible to show here that a small part of the H-atoms in C_2H_4 results from the linear carbonate constituent of the mixed solvent electrolyte. The C-atoms in CO mainly originated from EC but a noteworthy amount was also assigned to the decomposition of DEC. The decomposition of both carbonates contributed to the formation of CH_4. Nevertheless, more C-atoms originated from EC, whereas the main part of the H-atoms stemmed from the linear carbonate. Therefore, a far more complex mechanism must be behind this than simple separate decomposition reactions of the individual electrolyte constituents. The results indicate a potentially very interesting, not so far in literature reported reaction pathway that needs to be investigated in more detail. The C- and H-atoms in C_2H_6 can also originate from both carbonates. But the contribution of the H-atoms from linear carbonate predominates also in this case. These formations of reactive intermediates subject to C – H bond cleavage suggesting a radical type reaction especially for the linear carbonate, were not expected and provide a new basic approach for the consideration of decomposition reactions during SEI formation.

Furthermore, electrolyte mixtures with DMC or EMC instead of DEC and the effect of VC as additional film forming additive were investigated. The application of linear carbonates with methyl groups can noteworthy change the ratio of the C-atom

origin for the analyzed gases. Through the experiments with labeled components, the protective effects of VC suppressing the decomposition of other electrolyte components, in particular EC, could be demonstrated. The addition of VC resulted in a relatively decreased ratio of C-atoms originating from EC in the respective gaseous components.

Acknowledgements

The authors thank the German Federal Ministry of Education and Research (BMBF) for funding the project OptiZellForm (03XP0071B) within the ProZell cluster and the project HIT-Cell (03XP0113E) within Batterie2020. Open access funding enabled and organized by Projekt DEAL.

Conflict of Interest

The authors declare no conflict of interest.

Keywords: electrolyte · ethylene carbonate · gas analysis · GC-MS · lithium-ion battery · isotope labeling · NMC622 · solid-electrolyte interphase · SEI

[1] R. Schmuch, R. Wagner, G. Hörpel, T. Placke, M. Winter, *Nat. Energy* **2018**, *3*, 267–278.
[2] M. Winter, B. Barnett, K. Xu, *Chem. Rev.* **2018**, *118*, 11433–11456.
[3] M. Winter, *Z. Phys. Chem.* **2009**, *223*, 1395–1406.
[4] S. J. An, J. Li, C. Daniel, D. Mohanty, S. Nagpure, D. L. Wood, *Carbon* **2016**, *105*, 52–76.
[5] K. Xu, A. von Cresce, *J. Mater. Chem.* **2011**, *21*, 9849.
[6] M. Evertz, C. Lürenbaum, B. Vortmann, M. Winter, S. Nowak, *Spectrochim. Acta – Part B At. Spectrosc* **2015**, *112*, 34–39.
[7] S. Nowak, M. Winter, *Acc. Chem. Res.* **2018**, *5*, 265–272.
[8] S. Dühnen, J. Betz, M. Kolek, R. Schmuch, M. Winter, T. Placke, *Small Methods* **2020**, *4*, 2000039.
[9] I. Cekic-Laskovic, N. von Aspern, L. Imholt, S. Kaymaksiz, K. Oldiges, B. R. Rad, M. Winter, *Top. Curr. Chem.* **2017**, *375*, 1–64.
[10] K. Xu, *Chem. Rev.* **2004**, *104*, 4303–4418.
[11] K. Xu, *Chem. Rev.* **2014**, *114*, 11503–11618.
[12] L. El Ouatani, R. Dedryvère, C. Siret, P. Biensan, S. Reynaud, P. Iratçabal, D. Gonbeau, *J. Electrochem. Soc.* **2009**, *156*, A103–A113.
[13] M. Nie, J. Demeaux, B. T. Young, D. R. Heskett, Y. Chen, A. Bose, J. C. Woicik, B. L. Lucht, *J. Electrochem. Soc.* **2015**, *162*, A7008–A7014.
[14] J. Henschel, M. Dressler, M. Winter, S. Nowak, *Chem. Mater.* **2019**, *24*, 9970–9976.
[15] C. Korepp, H. J. Santner, T. Fujii, M. Ue, J. O. Besenhard, K.-C. Möller, M. Winter, *J. Power Sources* **2006**, *158*, 578–582.
[16] C. Yan, H. Yuan, H. S. Park, J.-Q. Huang, *J. Energy Chem.* **2020**, *47*, 217–220.
[17] S. Ma, M. Jiang, P. Tao, C. Song, J. Wu, J. Wang, T. Deng, W. Shang, *Prog. Nat. Sci.* **2018**, *28*, 653–666.
[18] T. Minato, T. Abe, *Prog. Surf. Sci.* **2017**, *92*, 240–280.
[19] M. Gauthier, T. J. Carney, A. Grimaud, L. Giordano, N. Pour, H.-H. Chang, D. P. Fenning, S. F. Lux, O. Paschos, C. Bauer, F. Maglia, S. Lupart, P. Lamp, Y. Shao-Horn, *J. Phys. Chem. Lett.* **2015**, *6*, 4653–4672.
[20] V. A. Agubra, J. W. Fergus, *J. Power Sources* **2014**, *268*, 153–162.
[21] C. P. Grey, J. M. Tarascon, *Nat. Mater.* **2016**, *16*, 45–56.
[22] P. Verma, P. Maire, P. Novák, *Electrochim. Acta* **2010**, *55*, 6332–6341.
[23] E. Peled, S. Menkin, *J. Electrochem. Soc.* **2017**, *164*, A1703–A1719.
[24] Y. P. Stenzel, F. Horsthemke, M. Winter, S. Nowak, *Separations* **2019**, *6*, 26.
[25] M. Metzger, B. Strehle, S. Solchenbach, H. A. Gasteiger, *J. Electrochem.* **2016**, *163*, A798–A809.
[26] T. Hatsukade, A. Schiele, P. Hartmann, T. Brezesinski, J. Janek, *ACS Appl. Mater. Interfaces* **2018**, *10*, 38892–38899.
[27] G. Gachot, P. Ribière, D. Mathiron, S. Grugeon, M. Armand, J.-B. Leriche, S. Pilard, S. Laruelle, *Anal. Chem.* **2011**, *83*, 478–485.
[28] M. Onuki, S. Kinoshita, Y. Sakata, M. Yanagidate, Y. Otake, M. Ue, M. Deguchi, *J. Electrochem.* **2008**, *155*, A794–A797.
[29] J.-P. Schmiegel, M. Leißing, F. Weddeling, F. Horsthemke, J. Reiter, Q. Fan, S. Nowak, M. Winter, T. Placke, *J. Electrochem. Soc.* **2020**, *167*, 60516.
[30] M. Leißing, M. Winter, S. Wiemers-Meyer, S. Nowak, *J. Chromatogr. A* **2020**, *1622*, 461122.
[31] X. Teng, C. Zhan, Y. Bai, L. Ma, Q. Liu, C. Wu, F. Wu, Y. Yang, J. Lu, K. Amine, *ACS Appl. Mater. Interfaces* **2015**, *7*, 22751–22755.
[32] F. Wang, F. Varenne, D. Ortiz, V. Pinzio, M. Mostafavi, S. Le Caër, *ChemPhysChem* **2017**, *18*, 2799–2806.
[33] W. Kong, H. Li, X. Huang, L. Chen, *J. Power Sources* **2005**, *142*, 285–291.
[34] C. Mao, R. E. Ruther, L. Geng, Z. Li, D. N. Leonard, H. M. Meyer, R. L. Sacci, D. L. Wood, *ACS Appl. Mater. Interfaces* **2019**, *11*, 43235–43243.
[35] M. R. Wagner, P. R. Raimann, A. Trifonova, K.-C. Moeller, J. O. Besenhard, M. Winter, *J. Electrochem. Soc.* **2004**, *7*, A201–A205.
[36] M. Winter, R. Imhof, F. Joho, P. Novák, *J. Power Sources* **1999**, *81–82*, 818–823.
[37] M. R. Wagner, P. R. Raimann, A. Trifonova, K.-C. Möller, J. O. Besenhard, M. Winter, *Anal. Bioanal. Chem.* **2004**, *379*, 272–276.
[38] M. Winter, P. Novák, *J. Electrochem.* **1998**, *145*, L27–L30.
[39] K. U. Schwenke, S. Solchenbach, J. Demeaux, B. L. Lucht, H. A. Gasteiger, *J. Electrochem.* **2019**, *166*, A2035–A2047.
[40] J. Henschel, C. Peschel, S. Klein, F. Horsthemke, M. Winter, S. Nowak, *Angew. Chem. Int. Ed.* **2020**, *59*, 6128–6137; *Angew. Chem.* **2020**, *132*, 6184–6193.
[41] C. Peschel, F. Horsthemke, M. Leißing, S. Wiemers-Meyer, J. Henschel, M. Winter, S. Nowak, *Batteries & Supercaps* **2020**, *3*, 1183–1192; Supercaps **2020**, 3, 1183–1192.
[42] B. Rowden, N. Garcia-Araez, *Energy Rep.* **2020**, *6*, 10–18.
[43] R. Nölle, K. Beltrop, F. Holtstiege, J. Kasnatscheew, T. Placke, M. Winter, *Mater. Today* **2020**, *32*, 131–146.
[44] F. Horsthemke, A. Friesen, X. Mönnighoff, Y. P. Stenzel, M. Grützke, J. T. Andersson, M. Winter, S. Nowak, *RSC Adv.* **2017**, *7*, 46989–46998.
[45] F. Horsthemke, A. Friesen, L. Ibing, S. Klein, M. Winter, S. Nowak, *Electrochim. Acta* **2019**, *295*, 401–409.
[46] D. Aurbach, B. Markovsky, I. Weissman, E. Levi, Y. Ein-Eli, *Electrochim. Acta* **1999**, *45*, 67–86.
[47] H. Ota, Y. Sakata, A. Inoue, S. Yamaguchi, *J. Electrochem.* **2004**, *151*, A1659–A1669.
[48] H. Yoshida, T. Fukunaga, T. Hazama, M. Terasaki, M. Mizutani, M. Yamachi, *J. Power Sources* **1997**, *68*, 311–315.
[49] G. M. Hobold, A. Khurram, B. M. Gallant, *Chem. Mater.* **2020**, *32*, 2341–2352.
[50] S. Leroy, F. Blanchard, R. Dedryvère, H. Martinez, B. Carré, D. Lemordant, D. Gonbeau, *Surf. Interface Anal.* **2005**, *37*, 773–781.
[51] S. Leroy, H. Martinez, R. Dedryvère, D. Lemordant, D. Gonbeau, *Appl. Surf. Sci.* **2007**, *253*, 4895–4905.
[52] T. Liu, L. Lin, X. Bi, L. Tian, K. Yang, J. Liu, M. Li, Z. Chen, J. Lu, K. Amine, K. Xu, F. Pan, *Nat. Nanotechnol.* **2019**, *14*, 50–56.

Manuscript received: August 10, 2021
Accepted manuscript online: August 11, 2021
Version of record online: August 25, 2021